

## Inter-Helix Distances in Lysophospholipid Micelle-Bound $\alpha$ -Synuclein from Pulsed ESR Measurements

Peter Borbat,<sup>†</sup> Trudy F. Ramlall,<sup>‡</sup> Jack H. Freed,<sup>\*,†</sup> and David Eliezer<sup>\*,‡</sup>

*Department of Chemistry and Biochemistry, Cornell University, Ithaca, New York 14853, and Department of Biochemistry and Program in Structural Biology, Weill Medical College of Cornell University, 1300 York Avenue, New York, New York 10021*

Received May 4, 2006; E-mail: dae2005@med.cornell.edu; jhf@ccmr.cornell.edu

The protein  $\alpha$ -synuclein ( $\alpha$ S) is linked to both sporadic and familial Parkinson's disease (PD) through its appearance in Lewy bodies (intraneuronal deposits that constitute a diagnostic hallmark of PD) and through several genetic polymorphisms (three point mutations and gene triplication or duplication) that lead to early onset disease.<sup>1</sup> Within Lewy bodies,  $\alpha$ S is found in highly ordered amyloid fibril aggregates, and PD-linked point mutations accelerate oligomerization of the protein *in vitro*,<sup>2</sup> suggesting that  $\alpha$ S toxicity may be linked to its aggregation. The normal function of  $\alpha$ S revolves around regulation of dopamine homeostasis and synaptic vesicle formation and fusion.<sup>3</sup> Dopamine has also been reported to directly influence  $\alpha$ S aggregation.<sup>4</sup> The functional association of  $\alpha$ S with dopamine combined with the fact that PD is fundamentally a dopamine deficit disorder suggests that the normal function of  $\alpha$ S may also play an important role in modulating the toxicity of the protein in disease.

$\alpha$ S undergoes a transition from a highly unstructured free state to a highly helical conformation upon binding to synthetic or brain-derived phospholipid vesicles, and the latter conformation is believed to mediate normal  $\alpha$ S functions. Detergent micelles induce a similar structural transition in  $\alpha$ S, and the sodium dodecyl sulfate (SDS) micelle-bound form of the protein has been used as a surrogate for the vesicle-bound state in a number of structural studies employing solution state NMR.<sup>5</sup> When bound to SDS micelles, the membrane-interacting N-terminal domain of  $\alpha$ S adopts two segments of helical structure separated by an ordered linker. The two helices are comprised of residues 3–37 and 45–92 and are oriented antiparallel to one another<sup>5c</sup> but do not contact each other.<sup>5d,e</sup>

Here we use pulsed dipolar ESR spectroscopy<sup>6</sup> to measure directly inter-helix distances in both SDS and lyso-1-palmitoylphosphotidylglycerol (LPPG) micelles. We show that distances can be measured with reasonable accuracy, and we establish a matrix of distances that characterizes the SDS micelle-bound state of the protein. When SDS is replaced with LPPG, we find that the two  $\alpha$ S helices splay further apart from each other, indicating that the relative positions of the helices depend on the topology of the surface they are bound to.

We generated 13 different double mutants of full length or C-terminally truncated  $\alpha$ S (the acidic C-terminus of the protein is not involved in lipid binding), each containing two cysteine residues using site-directed mutagenesis. One pair of cysteines was placed within a single helix to provide an internal distance control (H50C/T72C), two pairs were situated between the hinge region and each of the helices (E20C/S42C and S42C/E61C), and in the remaining cases, each cysteine was positioned in a different helix to report on an inter-helix distance (E35C/H50C, Q24C/E61C, E13C/T72C,

V3C/E83C, V3C/E61C, V3C/H50C, E13C/H50C, G31C/H50C, Q24C/Y72C, and Q24C/E83C). The first three inter-helix cysteine pairs were designed, based on our previous structural studies, so as to place the spin labels equidistant from the break between the two helices and also in the middle of the polar face of each helix, pointing directly away from the lipid bilayer. In addition to preventing potential effects on lipid binding, this design was intended to, as much as possible, keep the same relative orientation between each spin label and the associated helix axis. The expected relative positions of the different spin label pairs based on the previous NMR studies are schematically illustrated in Figure 1c.

The mutant proteins were expressed, purified, and modified quantitatively with the spin label methanethiosulfonate according to previously published protocols prior to the addition of SDS or LPPG.<sup>5d,6a</sup> Excess spin label was removed using a size exclusion spin column. The spin-labeled samples were then mixed with an equal volume of 80 mM SDS or LPPG prepared in the same buffer. Protein concentrations were in the range of  $60 \pm 30 \mu\text{M}$ . Glycerol (30 wt %) was added to the samples, which were then loaded into capillaries and flash frozen in liquid nitrogen. D<sub>2</sub>O, deuterated glycerol, and deuterated SDS (but not LPPG) were used in all cases. To minimize nuclear modulation effects caused by matrix deuterium nuclei, four-pulse double electron–electron resonance (DEER)<sup>6a,d,e,8</sup> was used in most cases at 17.4 GHz and 70 K on a specially constructed 2D FT-ESR spectrometer.<sup>7</sup> The results were consistent with those measured for several mutants with six-pulse double-quantum coherence (DQC) ESR.<sup>6a–c</sup> The protein concentrations used resulted in a high SNR, and the distance distributions and their averages were obtained through direct inversion of the time domain dipolar spectra by Tikhonov regularization.<sup>8</sup> The time domain and distance distribution data for the V3C/E83C mutant in both SDS and LPPG are shown in Figure 1. Data for the other double mutants and further experimental details are provided as Supporting Information.

The average distances measured between the different pairs of spin labels in the SDS and LPPG micelle-bound states are summarized in Table 1. The intra-helix distance measured between labels at positions 50 and 72 is very similar in both micelle types and only slightly larger than the expected distance of 33 Å, confirming the accuracy of the measurements.

All inter-helix distances confirm an antiparallel orientation of the two helices in both micelle types. For the SDS data, the distance between the two helices just outside the linker region (reflected in the 35–50 measurement of 24.7 Å) is consistent with approximately 7 residues in a nonhelical, somewhat extended conformation, in accord with NMR data.<sup>5</sup> Moving 11 residues further away from the linker along each helix leads to a distance of 40.5 Å between positions 24 and 61, indicating that the trajectory followed by the two helices places them considerably further apart from each other

<sup>†</sup> Cornell University.

<sup>‡</sup> Weill Medical College of Cornell University.

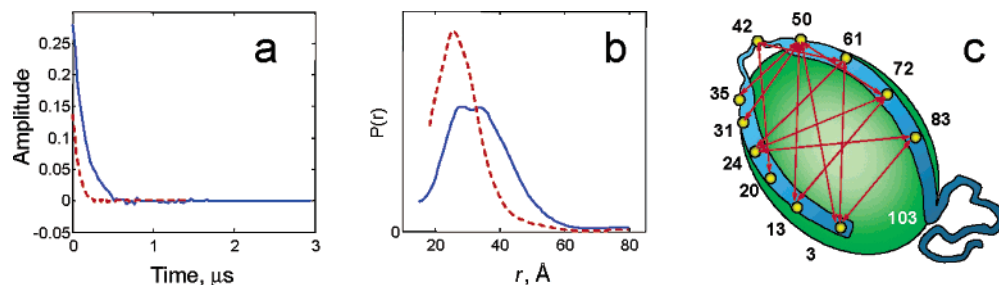


**Figure 1.** (a) Time domain dipolar signal with the background removed for the V3C/E83C mutant. Red (dashed) in SDS, blue (solid) in LPPG. (b) Distance distribution generated from (a) by Tikhonov regularization. (c) Cartoon representation of the two helices and linker region of  $\alpha$ S bound to an ellipsoidal micelle, illustrating the different distances measured using pulsed ESR.

**Table 1.** ESR Distance Measurements in Micelle-Bound  $\alpha$ S

labeled sites	SDS distance (Å)	LPPG distance (Å)
50/72	36	35
35/50	24.7	23.8
24/61	40.5	42.6
13/72	37	44
3/83	28.1	34.6
24/72	42.7	46
24/83	36.1	43.5
3/61	36	44.8
3/50	43	45
13/50	45	42.7
31/50	32.8	30.2
20/42	30	31.6
42/61	34.4	29.8

at this point. A further 11 residues along each helix, the distance between positions 13 and 72 is 37 Å, showing the helices remain far apart. Only when we get to the N-terminus of the first helix do the helices come nearer to each other once again, with a 28.1 Å distance between positions 3 and 83. The remaining inter-helical distances in SDS are also consistent with two well-separated antiparallel helices.

In the case of LPPG, the inter-helix distance nearest to the linker (positions 35–50) is 23.8 Å, essentially the same as that observed for the SDS case. The distance from positions 24 to 61 is 42.6 Å, slightly larger than that in the SDS case. Positions 13 and 72 are 44 Å apart, a full 7 Å further than that observed for SDS, and the distance between positions 3 and 83 is 34.6 Å, which is 6.5 Å larger than that in SDS. Thus, when bound to LPPG micelles, the two  $\alpha$ S helices are splayed further apart from each other than when bound to SDS micelles. The remaining inter-helix distances in the case of LPPG are generally consistent with a larger separation between the helices. Interestingly, the distance between position 42, within the linker region, and position 61 is shorter in LPPG than in SDS. This suggests that the relative positions of the linker and the second helix may also be somewhat different in the two micelles.

In SDS micelle-bound  $\alpha$ S, the two helices assume a well-defined position with respect to each other, which, in the absence of any inter-helix tertiary contacts, is presumed to be dictated by the trajectory of the ordered linker region. Our results, however, demonstrate that the relative position of the two helices is also sensitive to the composition of the bound micelle. LPPG differs from SDS both in its phosphatidylglycerol headgroup and in the length of its acyl chain, which contains four additional carbons. The local helical structure of the two micelle-bound  $\alpha$ S helices is unlikely to be sensitive to the nature of the micelle headgroups. Thus, the structural differences observed in LPPG-bound  $\alpha$ S may be a consequence either of a change in the local conformation of the linker region, which may be sensitive to the surrounding

headgroups, or of a difference in the size and/or geometry of the micelle formed by the longer LPPG acyl chains. The latter should lead to a micelle with a larger radius or major/minor semi-axes. Thus, an appealing explanation for our data is that the topology of micelle-bound  $\alpha$ S is determined by that of the bound micelle. For the smaller SDS micelles, the ends of the two helices are constrained to approach each other by the limited micelle surface area. For LPPG, the larger micelle allows the helices to splay further apart on its surface.

Ultimately, the question of most interest is what happens to the topology of  $\alpha$ S when it is bound to synaptic vesicles. The current work demonstrates that pulsed ESR distance measurements could provide such information and establishes a framework for the comparison of the micelle- and vesicle-bound protein.

**Acknowledgment.** This work was supported by grants from the NIH/NIA (AG019391 to D.E.), NIH/NCRR (P41-RR016292 to J.H.F.), and NIH/NIBIB (EB03150 to J.H.F.).

**Supporting Information Available:** Further experimental details and time-domain dipolar spectrum and distance distributions for other double mutants. This material is available free of charge via the Internet at <http://pubs.acs.org>.

## References

- (1) Moore, D. J.; West, A. B.; Dawson, V. L.; Dawson, T. M. *Annu. Rev. Neurosci.* **2005**, *28*, 57–87. (b) Lundvig, D.; Lindersson, E.; Jensen, P. H. *Brain Res. Mol. Brain Res.* **2005**, *134*, 3–17.
- (2) (a) Conway, K. A.; Harper, J. D.; Lansbury, P. T. *Nat. Med.* **1998**, *4*, 1318–1320. (b) Narhi, L.; Wood, S. J.; Steavenson, S.; Jiang, Y.; Wu, G. M.; Anafi, D.; Kaufman, S. A.; Martin, F.; Sitney, K.; Denis, P.; Louis, J.-C.; Wypych, J.; Biere, A. L.; Citron, M. *J. Biol. Chem.* **1999**, *274*, 9843–9846. (c) Greenbaum, E. A.; Graves, C. L.; Mishizen-Eberz, A. J.; Lupoli, M. A.; Lynch, D. R.; Englander, S. W.; Axelsen, P. H.; Giasson, B. I. *J. Biol. Chem.* **2005**, *280*, 7800–7807.
- (3) (a) Sidhu, A.; Wersinger, C.; Vernier, P. *FASEB J.* **2004**, *18*, 637–647. (b) Chandra, S.; Gallardo, G.; Fernandez-Chacon, R.; Schluter, O. M.; Sudhof, T. C. *Cell* **2005**, *123*, 383–396.
- (4) Conway, K. A.; Rochet, J. C.; Bieganski, R. M.; Lansbury, P. T., Jr. *Science* **2001**, *294*, 1346–1349.
- (5) (a) Eliezer, D.; Kutluay, E.; Bussell, R., Jr.; Browne, G. *J. Mol. Biol.* **2001**, *307*, 1061–1073. (b) Bussell, R., Jr.; Eliezer, D. *J. Mol. Biol.* **2003**, *329*, 763–778. (c) Chandra, S.; Chen, X.; Rizo, J.; Jahn, R.; Sudhof, T. C. *J. Biol. Chem.* **2003**, *278*, 15313–15318. (d) Bussell, R., Jr.; Ramlall, T. F.; Eliezer, D. *Protein Sci.* **2005**, *14*, 862–872. (e) Ulmer, T. S.; Bax, A.; Cole, N. B.; Nussbaum, R. L. *J. Biol. Chem.* **2005**, *280*, 9595–9603. (f) Bisaglia, M.; Tessari, I.; Pinato, L.; Bellanda, M.; Giraud, S.; Fasano, M.; Bergantino, E.; Bubacco, L.; Mammì, S. *Biochemistry* **2005**, *44*, 329–339. (g) Ulmer, T. S.; Bax, A. *J. Biol. Chem.* **2005**, *280*, 43179–43187.
- (6) (a) Berliner, L. J.; Eaton, G. R.; Eaton, S. S., Eds. *Biological Magnetic Resonance*; Kluwer-Plenum: New York, 2000; Vol. 21. (b) Borbat, P. P.; Freed, J. H. *Chem. Phys. Lett.* **1999**, *313*, 145–154. (c) Borbat, P. P.; Mchaourab, H. S.; Freed, J. H. *J. Am. Chem. Soc.* **2002**, *124*, 5304–5314. (d) Milov, A. D.; Maryasov, A. G.; Tsvetkov, Y. D. *Appl. Magn. Reson.* **1998**, *15*, 107–143. (e) Pfannebecker, V.; Klos, H.; Hubrich, M.; Volkmer, T.; Heuer, A.; Wiesner, U.; Spiess, H. W. *J. Phys. Chem.* **1996**, *100*, 13428–13432.
- (7) Borbat, P. P.; Crepeau, R. H.; Freed, J. H. *J. Magn. Reson.* **1997**, *127*, 155–167.
- (8) Chang, Y.-W.; Borbat, P. P.; Freed, J. H. *J. Magn. Reson.* **2005**, *172*, 279–295.

JA063122L